2018 3rd International Electrical Engineering Conference (IEEC 2018)
Feb, 2018 at IEP Centre, Karachi, Pakistan

A Validity of Transparency Optimized 4-Channel Architecture in Bilateral Teleoperation

Muhammad Hammad Saleem* and Riaz Uddin

Department of Electrical Engineering, NED University of Engineering and Technology,
Karachi, 75290, Pakistan (hammadsaleem@neduet.edu.pk; riazuddin@neduet.edu.pk) * Corresponding author

Abstract: In order to perform any task remotely using teleoperation system, transparency is considered as an important performance measure. There are many teleoperation architectures, which are used in several applications of teleoperation. In this research, 4-channel architecture is analyzed and validated as it provides adequate number of parameters for achieving better transparency as compared to other teleoperation architectures. Initially, transparency index is defined then further expressions for hybrid parameters are derived. Later, controller gains are designed to achieve good transparency. Force and position profiles of the master and slave devices showing transparency improvement are obtained by the help of Matlab/Simulink with/without time delay. The controllers are designed in such a way that the required number of sensors are used as minimum as possible.

Keywords: 4-Channel architecture, Transparency index, Teleoperation

I. INTRODUCTION

For high-fidelity teleoperation, transparency of the master–slave system is necessary. Therefore, as a performance measure, transparency is defined as "*the description of the degree of telepresence of the remote site available to the human operator through the tele-operator device*" [1]. For bilaterally controlled teleoperation, transparency is determined by the reflection of slave/environment interaction forces to the user's hand by the master device[2].

II. TRANSPARENCY IN HAPTIC TELEOPERATION

Let f_h be the hand/master interaction force and f_e be the slave/environment interaction force, the dynamics of the master and the slave can be written as[3]:

$$f_m + f_h = M_m\ddot{x}_m + B_m\dot{x}_m = M_m\dot{v}_m + B_m v_m, \quad (1)$$

$$f_s - f_e = M_s\ddot{x}_s + B_s\dot{x}_s = M_s\dot{v}_s + B_s v_s. \quad (2)$$

Where: $M_m, M_s, f_m, f_s, x_m, x_s, v_m, v_s$ are master inertia, slave inertia, master force, slave force, master position, slave position, master velocity and slave velocity respectively.

For the ideal transparency, master position (x_m) must be matched with the slave position $(x_s)$and human force (f_h) must be matched with the environment force (f_e)[4] as follows:

$$x_m = x_s \quad (3)$$

$$f_h = f_e \quad (4)$$

The teleoperation system can be represented by an equivalent diagram according to [1] as shown in Fig. 1.

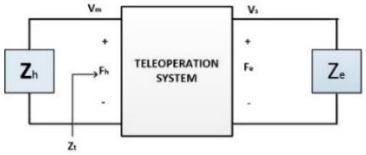

Fig. 1 Equivalent circuit representation of a teleoperation system[1].

Here, Z_h, Z_e and Z_t are dynamics of human operator hand, remote environment and transmitted impedance.

For the evaluation of transparency of teleoperation, the another appropriate way to represent is the two port network of teleoperation system [5] (as shown in Fig. 1) is to represent it by the hybrid matrix.

$$\begin{bmatrix} F_h \\ -v_s \end{bmatrix} = \begin{bmatrix} h_{11} & h_{12} \\ h_{21} & h_{22} \end{bmatrix} \begin{bmatrix} v_m \\ F_e \end{bmatrix} \quad (5)$$

For the ideal transparency, the hybrid matrix must look like:

$$\begin{bmatrix} h_{11} & h_{12} \\ h_{21} & h_{22} \end{bmatrix} = \begin{bmatrix} 0 & 1 \\ -1 & 0 \end{bmatrix} \quad (6)$$

III. HYBRID MATRIX PARAMETERS

A. Hybrid Parameters For 4C-Architecture

In this section, the individual definition and physical meaning of hybrid parameters are discussed as below:

i. $\boldsymbol{h_{11} = \frac{F_h}{V_m}|F_{e=0}}$

h_{11} represents the free motion behavior of input impedance as environment force(F_e) is equal to zero. It also tells that what human operator feels in free motion by moving master arm [2].

In order to achieve ideal transparency of teleoperation, we need to derive the relationships of the hybrid matrix. From Fig. 2, we can write the following equations:

$$F_h + F_h C_6 - V_m C_m - F_e C_2 e^{-std} - V_s C_4 e^{-std} = V_m \quad (7)$$

$$V_m C_1 e^{-std} + F_h C_3 e^{-std} - F_e C_5 - F_e - V_s C_s = V_s Z_s \quad (8)$$

For calculating h_{11}, separating V_s from Eq. (8), $F_e = 0$ and put into the Eq. (7), we get:

$$\boxed{h_{11} = \frac{F_h}{V_m} = \frac{Z_{sc}Z_{mc} + C_1 C_4 e^{-2std}}{Z_{sc}(1+C_6) - C_3 C_4 e^{-2std}}} \quad (9)$$

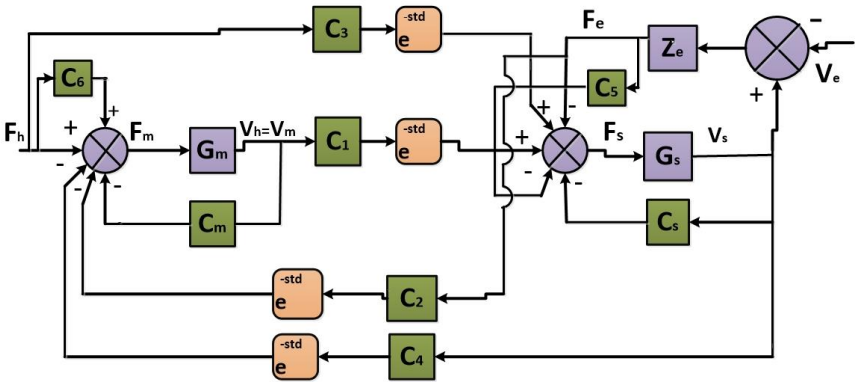

Fig.2 Block Diagram Representation of 4-Channel Architecture

where,

$Z_s = \frac{1}{G_s}, Z_m = \frac{1}{G_m}, Z_{sc} = Z_s + C_s,$

$Z_s = M_s s + B_s, C_s = \frac{K_{ps}}{s} + K_{d_s},$

$Z_{mc} = Z_m + C_m, Z_m = M_m s + B_m,$

$C_m = \frac{K_{pm}}{s} + K_{d_m}, td = communication\ delay$

ii. $\boldsymbol{h_{12} = \frac{F_h}{F_e}|V_{m=0}}$

h_{12} is a measure of force tracking for the haptic teleoperation system when the master is in fixed position[2]. It also tells that what human operator feels in contact motion. For calculating h_{12}, separating V_s from eq. (8), put $V_m = 0$ and put into the Eq. (7), we get:

$$h_{12} = \frac{F_h}{F_e} = \frac{C_2 e^{-std} Zsc - (1+C_5) C_4 e^{-std}}{Zsc(1+C_6) - C_3 C_4 e^{-2std}} \quad (10)$$

iii. $\boldsymbol{h_{21} = -\frac{V_s}{V_m}|F_{e=0}}$

h_{21} is a measure of position (velocity) tracking performance when the slave does not come in contact with the environment (free space condition) . It also tells that how well slave follow the master position in free motion.

For calculating h_{21}, separating F_h from Eq. (8), put $F_e = 0$ and put into the Eq. (7), we get:

$$h_{21} = -\frac{V_s}{V_m} = -\frac{C_1(1+C_6)e^{-std} + Z_{mc}C_3 e^{-std}}{Z_{sc}(1+C_6) - C_4 C_3 e^{-2std}} \quad (11)$$

iv. $\boldsymbol{h_{22} = -\frac{V_s}{F_e}|V_{m=0}}$

h_{22} is the output admittance when the master is fixed in position. It also tells that how well master/slave is locked in contact mode.

For calculating h_{22}, separating F_h from Eq. (8), put $V_m = 0$ and put into the Eq. (7), we get:

$$h_{22} = -\frac{V_s}{F_e} = \frac{-C_2 C_3 e^{-2std} + (1+C_5)(1+C_6)}{[-C_4 C_3 e^{-2std} + Z_{sc}(1+C_6)]} \quad (12)$$

From eq. (9) ~ (12), we get:

$$\begin{bmatrix} h_{11} & h_{12} \\ h_{21} & h_{22} \end{bmatrix} = \begin{bmatrix} \frac{Z_{sc}Z_{mc} + C_1 C4 e^{-2std}}{Z_{sc}(1+C_6) - C_3 C_4 e^{-2std}} & \frac{C_2 Zsc e^{-std} - (1+C_5) C_4 e^{-std}}{Zsc(1+C_6) - C_3 C_4 e^{-2std}} \\ -\frac{C_1(1+C_6)e^{-std} + Z_{mc}C_3 e^{-std}}{Z_{sc}(1+C_6) - C_4 C_3 e^{-2std}} & \frac{-C_2 C_3 e^{-2std} + (1+C_5)(1+C_6)}{[-C_4 C_3 e^{-2std} + Z_{sc}(1+C_6)]} \end{bmatrix}$$

Put td=0 in the above matrix to obtain the hybrid matrix without communication delay

$$\begin{bmatrix} h_{11} & h_{12} \\ h_{21} & h_{22} \end{bmatrix} = \begin{bmatrix} \frac{Z_{sc}Z_{mc} + C_1 C4}{Z_{sc}(1+C_6) - C_3 C_4} & \frac{C_2 Zsc - (1+C_5) C_4}{Zsc(1+C_6) - C_3 C_4} \\ -\frac{C_1(1+C_6) + Z_{mc}C_3}{Z_{sc}(1+C_6) - C_4 C_3} & \frac{-C_2 C_3 + (1+C_5)(1+C_6)}{[-C_4 C_3 + Z_{sc}(1+C_6)]} \end{bmatrix} \quad (13)$$

B. Selection of Controller gains for Ideal Transparency of 4-Channel Architecture:

If we compare Eq. (6) and eq. (13), we can select the relations of C_1, C_2, C_3 and C_4 in terms of C_5, C_6, Z_{sc}, Z_{mc} to achieve good transparency of teleoperation.

From eq. (6), h_{11}=0 which gives $Z_{sc}Z_{mc} + C_1 C_4$ =0. Now by selecting the following relations of C_1 and C_4 in terms of $Z_{sc}$and Z_{mc}, we can achieve the ideal transparency as [2]:

$C_1 = Z_{sc} = Z_{s+} C_s$ (14)

$C_4 = -Z_{mc} =$ - $(Z_m + C_m)$ (15)

From eq. (6), h_{22}=0 which gives $-C_2 C_3 + (1 + C_5)(1 + C_6) = 0$

For ideal transparency,

$C_2 = (1 + C_6)$ (16)

$C_3 = (1 + C_5)$ (17)

IV. SIMULATION

A. Simulation Scenario

The simulation of 4C-architecture is done in Matlab/Simulink by implementing an equivalent 4channel teleoperation model according to Fig. 2. A benchmark test of free and contact motion is performed and force and position profiles are depicted. Details of Parameters of master and slave devices are mentioned in Table I.

Table I Parameters of master, slave devices and environment

Parameters	Master device	Slave device	Environment
Mass (M_m, M_s, M_e)	0.1 Kg	0.1 Kg	Negligible
Damper(B_m, B_s, B_e)	0.001 $N.s/mm$	0.001 $N.s/mm$	Negligible
Spring constant(K_m, K_s, K_e)	Negligible	Negligible	*5 N/mm*

There are 4 controllers (C_1 to C_4) connected in 4-channel architecture including two compensators named C_6 and C_5. Among C_1 to C_6 controllers/compensators, C_6 and C_5 are master and slave local force compensators, respectively[6]. C_m and C_s are master local velocity controller and slave local velocity controller [6] respectively. C_2 and C_3 are used to measure the contact forces of the remote side. The measured master and slave velocities are passed through the impedance filters (C_1V_h and C_4Ve) to convert them into forces[6].

Table II shows the gains of all the controller and compensators which are set according to Eqs. (14) ~ (17).

Table II Controller gains and justifications according to transparency index

Controllers/ Compensators	Formulas	Gains
C_m	$\frac{K_{p_m}}{s} + K_{d_m}$	$\frac{25}{s} + 3$
C_s	$\frac{K_{p_s}}{s} + K_{d_s}$	$\frac{50}{s} + 7$
C_1	$Z_s + C_s = (M_s s + B_s) + (\frac{K_{p_s}}{s} + K_{d_s})$	$0.1s + 8 + \frac{50}{s}$
C_2	$1 + C_6$	0
C_3	$1 + C_5$	1
C_4	$-(Z_m + C_m) = -(M_m s + B_m) - (\frac{K_{p_m}}{s} + K_{d_m})$	$-0.1s - 4 - \frac{25}{s}$
C_5	$C_3 - 1$	0
C_6	$C_2 - 1$	-1

In our simulation model, C_5=0 which provides the gain of C_3=1, whereas C_6=-1 which implies that C_2=0 therefore there will be no need of the force measurement sensor on the slave side[5]

B. Simulation Results and Discussion

The simulation model provided the position and force profiles in free and contact motion both in the absence and presence of time delays (as shown in Fig. 4 and Fig. 5).

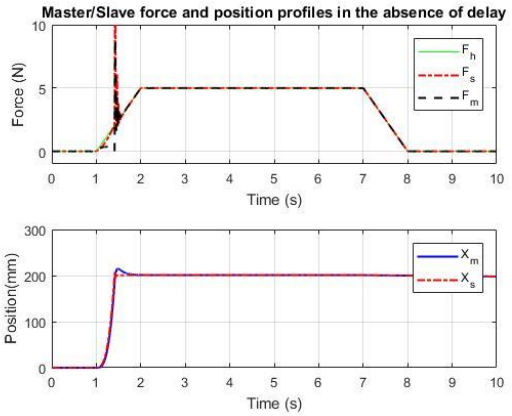

Fig. 4 Position and force profiles of master/ slave devices in the absence of time delay

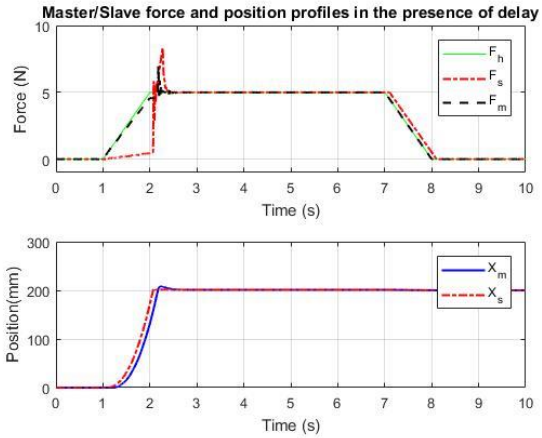

Fig. 5 Position and force profiles of master/ slave devices in the presence of time delay

From Fig. 4, we can conclude that free motion and contact mode starts from 1 to 1.5 *seconds* and 1.5 to 8 *seconds*, respectively. The human operator input force F_h= *5N* is applied at the master side in the form of trapezoidal pulse from t = 1 to 8*secs*. This simulation is done initially for no time delay, where master force tracks the slave with initial contact oscillations as the slave comes in contact with the environment at *200mm* (as shown in the upper plot of fig. 4). The lower plot in fig. 4 shows the position tracking, where in free motion (before 1.5 *secs*) the slave tracks the master well and after making contact at 1.5 *seconds*, there is a small error between x_m and x_s which is synchronized with force tracking in contact mode as can be seen in upper plot of Fig. 4.

Similarly, the force and position tracking is done in the presence of communication delay (100 *msec*) as shown in Fig. 5. In the presence of delay, the contact motion occurs at 2.2 *seconds*. When the slave comes in contact with the environment, there is a jerk in the master and slave forces. The position profile in the lower plot of Fig. 5 shows that due to the time delay, there is an error between master and slave positions x_m and x_s respectively in the free motion condition. When the slave comes in contact with the environment at *200mm* then there is a small error between x_m and x_s which dies out very quickly.

V. CONCLUSION

4-channel architecture is validated in a Matlab/Simulink model to show better transparency in the behavior of master and slave devices. The magnitude of the position error is negligible even when the time delay is considered in the simulation model. According to ideal transparency index, different controllers/compensators are designed and validated such that there is no need of force measurement on the slave side by getting reduced number of sensors usage.

REFERENCES

[1] Lawrence, D.A., *Stability and transparency in bilateral teleoperation.* IEEE transactions on robotics and automation, 1993. **9**(5): p. 624-637.

[2] Tavakoli, M., et al., *High-fidelity bilateral teleoperation systems and the effect of multimodal haptics.* IEEE Transactions on Systems, Man, and Cybernetics, Part B (Cybernetics), 2007. **37**(6): p. 1512-1528.

[3] Uddin, R. and J. Ryu, *Predictive control approaches for bilateral teleoperation.* Annual Reviews in Control, 2016. **42**: p. 82-99.

[4] Uddin, R., S. Park, and J. Ryu, *A predictive energy-bounding approach for Haptic teleoperation.* Mechatronics, 2016. **35**: p. 148-161.

[5] Hashtrudi-Zaad, K. and S.E. Salcudean, *Analysis of control architectures for teleoperation systems with impedance/admittance master and slave manipulators.* The International Journal of Robotics Research, 2001. **20**(6): p. 419-445.

[6] Hashtrudi-Zaad, K. and S.E. Salcudean, *Transparency in time-delayed systems and the effect of local force feedback for transparent teleoperation.* IEEE Transactions on Robotics and Automation, 2002. **18**(1): p. 108-114.